Research Square

Preprints are preliminary reports that have not undergone peer review.
They should not be considered conclusive, used to inform clinical practice,
or referenced by the media as validated information.

Comparative Numerical Evaluation of the Seismic Behavior of the Steel Framing System and Confined Masonry for a Single-Family Dwelling in Peru: A Computational Modeling Study

JULIAN ÑAUPA TAPULLIMA
Universidad Autónoma del Perú
PAUL RICARDO PRUDENCIO GALVEZ
pprudencio@autonoma.edu.pe

Universidad Autónoma del Perú

Systematic Review

Keywords: steel framing, confined masonry, seismic analysis, ETABS 22, interstory drift, E.030, computational modeling

Posted Date: August 11th, 2026

DOI: https://doi.org/10.21203/rs.3.rs-10383738/v1

License: This work is licensed under a Creative Commons Attribution 4.0 International License.
Read Full License

Additional Declarations: No competing interests reported.

Abstract

This study numerically evaluated the seismic behavior of the Steel Framing construction system compared to confined masonry for a single-family dwelling in a seismic zone of Peru, using computational simulation rather than physical testing. The research applied a quantitative approach with a non-experimental, cross-sectional, descriptive-comparative design. Two three-dimensional models were built in ETABS 22 through the Python COM API: a 6.00 m × 4.00 m Steel Framing module with ASTM A446 Gr.C profiles, and a confined masonry module of the same footprint with f'c = 175 kgf/cm² columns and f'm = 65 kgf/cm² walls. Results showed that confined masonry exhibited greater lateral rigidity (T1 = 0.150 s vs. T1 = 0.280 s for Steel Framing), maximum interstory drifts of 0.0031 and 0.0048 respectively — both within the E.030 limit of 0.005 — and 32.3% higher base shear than Steel Framing. Both systems satisfied the seismic safety criteria of the E.030 Standard within the specific geometric and soil conditions modeled. Within these limits, Steel Framing behaves as a technically viable lightweight structural alternative for single-story housing in the seismic zone analyzed; broader claims regarding construction speed and cost, reported elsewhere in the literature, were not evaluated in this study and are not asserted as findings here.

1. INTRODUCTION

Peruvian territory lies within the Pacific Ring of Fire, one of the most seismically active zones on the planet (CENEPRED, 2014). This condition poses a permanent threat to the population, especially in Lima and other coastal and Andean areas, where most of the country's housing stock is concentrated. In this context, the choice of construction system for single-family dwellings constitutes a critical engineering decision that must balance seismic safety, economic feasibility, and construction speed.

Prefabricated modular Steel Framing homes, based on cold-formed light-gauge galvanized steel profiles (ASTM A446 Gr.C), have been proposed as a technically viable lightweight construction solution (Dannemann, 2007). As an alternative, confined masonry remains the predominant conventional system in Peru, governed by specifications E.060 and E.070 of the National Building Code (RNE), with brick load-bearing walls and reinforced-concrete confining columns.

A direct technical comparison between Steel Framing and reinforced-concrete or masonry systems under seismic loading, using computational modeling in structural analysis software, has been reported for regular structures in the Latin American context (Chávez Amaguaña et al., 2022), finding that Steel Framing structures can be substantially lighter than reinforced-concrete equivalents, with corresponding effects on seismic demand. However, a systematic comparative evaluation of Steel Framing and confined masonry under the specific parameters of Peru's E.030 standard — through three-dimensional computational modeling — represents a methodological gap that this research seeks to fill, providing numerical evidence directly traceable through the ETABS 22 COM API.

Comparison through computational modeling makes it possible to quantify differences in seismic performance in terms of interstory drift, modal periods, base shear, and internal forces, contributing to

evidence-based technical decision-making. Numerical and experimental studies of cold-formed steel wall systems support their consideration as a viable lateral-load-resisting mechanism: the hysteretic model developed by Nithyadharan and Kalyanaraman (2012) showed that cold-formed steel wall panels can exhibit stable, ductile behavior under cyclic loading; full-scale cyclic testing of strap-braced cold-formed steel walls by Al-Kharat and Rogers (2007) quantified their inelastic performance and ductility under capacity-based design; and Moghimi and Ronagh (2009) evaluated multiple strap-bracing arrangements experimentally, identifying failure modes and detailing improvements that promote ductile, non-brittle response.

This research is justified because it provides quantitative, comparative evidence — obtained entirely through desk-based computational simulation, without physical prototypes — that can inform engineers, builders, and decision-makers regarding the seismic behavior of Steel Framing relative to confined masonry in the Peruvian regulatory context, within the scope of the geometry and conditions modeled. The study offers technical convenience by providing traceable modeling data, social relevance by addressing the safety of housing in at-risk areas, theoretical value by contrasting seismic behavior between systems, and methodological usefulness by developing a replicable comparison protocol using the COM API.

The research question is: To what extent does the seismic behavior of the Steel Framing system differ from that of the confined masonry system for a single-family dwelling under the parameters of the E.030 Standard? The general objective is to evaluate the structural behavior of the Steel Framing system compared to confined masonry for a single-family dwelling in a seismic zone, in accordance with the E.030 Standard. The specific objectives are: (1) define the seismic and geotechnical parameters of the site in accordance with E.030; (2) build three-dimensional structural models of each system in ETABS 22 using the Python COM API; (3) compare interstory drifts, modal periods, and internal forces; and (4) determine the advantages and limitations of each system based on regulatory seismic performance indicators, strictly within the scope of the models developed.

2. METHODOLOGY

2.1 Type and Design of the Research

The research was applied in type, aimed at solving the problem of comparing seismic performance between construction systems for housing in Peru through computational (desk-based) modeling. The approach was quantitative, based on the analysis of numerical data from computational simulations; no physical prototype was built or tested. The design was non-experimental, cross-sectional, descriptive-comparative, since data were collected and compared at a single point in time without manipulating the independent variables (construction systems), but rather observing and measuring the structural responses — drifts, periods, and internal forces — under the same seismic loading conditions defined by the E.030 Standard (Hernández-Sampieri & Mendoza, 2018).

2.2 Population, Sample, and Sampling

The population consisted of the set of theoretical structural models of single-story single-family dwellings built under the Steel Framing and confined masonry systems using Peruvian regulatory parameters. The sample was non-probabilistic by convenience, selecting one prototype per system: a 6.00 m × 4.00 m × 2.40 m Steel Framing module with ASTM A446 Gr.C profiles, and a confined masonry module of the same dimensions with 15×15 cm columns of f'c = 175 kgf/cm² and walls of f'm = 65 kgf/cm². Both units were located on type S2 soil in Lima (Z = 0.35, U = 1.0, S = 1.15) in accordance with the E.030-2018 standard.

The 6.00 m × 4.00 m module corresponds to a minimum functional single-story housing cell consistent with the dimensions typically used in Peruvian social-interest housing and with the basic single-module comparative approach applied in regional Steel Framing versus reinforced-concrete/masonry studies (Chávez Amaguaña et al., 2022). The 2.40 m clear height meets the minimum regulatory requirement for single-family dwellings under the RNE. By keeping the geometry, seismic zone, and loads constant, the effect of the construction system as the independent variable on seismic behavior as the dependent variable is isolated. This single-prototype, single-story convenience sample is a deliberate scope boundary of the study and is addressed explicitly in the Limitations (Section 4).

2.3 Variables and Operationalization

The independent variable was the construction system (Steel Framing vs. confined masonry), operationalized through the selection of the type of system applied to each prototype: ASTM A446 Gr.C profiles for Steel Framing, or columns of f'c = 175 kgf/cm² and walls of f'm = 65 kgf/cm² for confined masonry, modeled in ETABS 22 for a 6.00 m × 4.00 m × 2.40 m module under the same seismic parameters of the E.030 Standard.

The dependent variable was the seismic behavior of the single-family dwelling, operationalized through the quantitative indicators extracted from the ETABS 22 analysis: interstory drift (Δ/H), modal periods (T1–T6), cumulative participating masses, base shear (Vx, Vy), axial force (P), shear (V2), and bending moment (M3) in columns or equivalent studs, verified against the limits of the E.030 Standard.

2.4 Instruments and Materials

The following were used: (a) ETABS 22 software for three-dimensional modeling and seismic analysis; (b) Python 3.11 with the ETABS COM API for modeling automation and results extraction; (c) regulatory data collection sheets in Microsoft Excel to record parameters from E.030, E.020, E.070, and E.060; (d) technical catalogs of ASTM A446 Gr.C and IRAM-IAS U-500-205 galvanized steel profiles; (e) the RNE materials library for properties of f'c = 175 kgf/cm² concrete and f'm = 65 kgf/cm² masonry; and (f) AutoCAD software for producing technical drawings of both modules.

2.5 Procedure

The procedure was carried out entirely in gabinete (desk-based computational work), in four sequential phases. In the first phase — parameter definition — the seismic parameters were extracted in

accordance with E.030-2018: Z = 0.35 (Zone 3), U = 1.00 (Category C), S = 1.15 (S2), Tp = 0.60 s, TL = 2.00 s, R = 3.00 (confined masonry), and R = 8.00 (Steel Framing — rolled/cold-formed steel).

In the second phase — modeling — the three-dimensional geometry of each system was built in ETABS 22. For Steel Framing, C100×50×1.5 mm profiles were defined as studs and U100×40×0.9 mm profiles as tracks, spaced at 0.60 m. For confined masonry, 6 columns of 15×15 cm, 6 tie beams of 15×20 cm, and 5 load-bearing walls with e = 15 cm were defined. Both models used the same 6.00 × 4.00 × 2.40 m module and the kN-m-°C unit system.

In the third phase — analysis — modal analysis (12 modes), CQC spectral analysis in accordance with E.030, equivalent static analysis, and LRFD and ASD load combinations were performed. The extracted parameters included: periods T1 through T6, cumulative participating masses, interstory drifts in X and Y, base shear Vx and Vy, and internal forces P, V2, and M3 in columns. In the fourth phase — comparison — the results of both models were processed in Python using the NumPy, Pandas, and Matplotlib libraries, generating comparative charts for each seismic performance indicator, all original and produced by the authors from the ETABS output.

2.6 Data Analysis

Data analysis was carried out using quantitative structural engineering techniques. Interstory drifts were checked against the $\Delta/H \leq 0.005$ limit of the E.030 Standard for both systems. Modal periods and cumulative participating masses were evaluated to verify compliance with the 90% minimum required by E.030. Internal forces in columns were analyzed using the LRFD method in accordance with AISC 360 – 16 for Steel Framing and the ultimate strength method in accordance with E.060 for masonry. Results were organized into comparative tables and represented graphically through bar charts, drift profiles, and performance radar charts generated with Matplotlib.

2.7 Ethical Considerations

The research was conducted under principles of originality and academic honesty in accordance with the guidelines of Universidad Autónoma del Perú. Proper citation of bibliographic sources was ensured, respecting the intellectual property of the standards and software used. The study used only public regulatory data and the authors' own computational models; it did not involve human or animal subjects, personal data, or physical testing, and therefore required no ethics committee approval or participant consent (see Declarations).

3. RESULTS

The results are presented in correspondence with the specific objectives. They are organized into five subsections covering the general comparative analysis, interstory drifts, modal periods and masses, forces in columns, and the performance summary table. All numerical values were extracted directly from ETABS 22 via the Python COM API (TableKey: "Modal Participating Mass Ratios," "Story Drifts,"

"Frame Forces"), ensuring direct traceability between the computational model and the data presented. All figures were produced by the authors in Matplotlib from this ETABS output.

3.1 Regulatory Parameters and Mechanical Properties of Materials

Table 1. *E.030 regulatory parameters for structural modeling in ETABS 22*

Parameter	Confined Masonry	Steel Framing
Zone factor Z	0.35	0.35
Usage category U	1.00	1.00
Soil factor S (S2)	1.15	1.15
Corner period Tp (s)	0.60	0.60
Period TL (s)	2.00	2.00
Reduction coefficient R	3.00	8.00
Seismic zone	Z3 — Lima	Z3 — Lima

Note. Source: Ministry of Housing, Construction and Sanitation (2018). Technical Standard E.030 — RNE. Prepared by the authors.

The comparative dashboard generated in ETABS 22 made it possible to simultaneously assess the six main seismic performance indicators: drifts in X and Y, modal periods, base shear, axial forces, and the global performance radar chart. The results revealed that confined masonry exhibited greater rigidity and smaller drifts, while Steel Framing showed greater flexibility and lower seismic mass in action, with both systems meeting the E.030 regulatory limits within the geometry modeled.

3.2 Interstory Drifts

Figures 1 and 2 show the interstory drift profiles in the X and Y directions. The reference line indicates the maximum permissible limit of 0.005 established by the E.030 Standard (the more restrictive limit, applied to both systems to ensure comparability).

Table 2. *Maximum interstory drifts by direction — E.030 regulatory comparison (single-story module)*

Direction	Confined Masonry	Steel Framing	E.030 Limit	Compliant?
X	0.0031	0.0048	≤ 0.005	Yes / Yes
Y	0.0029	0.0046	≤ 0.005	Yes / Yes

Note. Values expressed as the Δ/H ratio (dimensionless), for the single story modeled. Prepared by the authors using ETABS 22 and Python Matplotlib.

The drifts in the X direction show that confined masonry recorded a maximum drift of 0.0031 (62% of the regulatory limit), while Steel Framing reached 0.0048 (96% of the limit), with a significantly smaller safety margin, though without exceeding it. In the Y direction, results are consistent: both systems comply with the E.030 limit, with confined masonry recording a smaller drift (0.0029 vs. 0.0046, a 35.4% difference to the disadvantage of Steel Framing). The consistency in both directions confirms that the seismic behavior shows no plan irregularities within the model.

3.3 Modal Periods and Masses

The modal analysis revealed significant differences between the two systems. Confined masonry showed a fundamental period T1 = 0.150 s, compared to T1 = 0.280 s for Steel Framing, representing an 86.7% difference that quantifies the greater lateral rigidity provided by the load-bearing walls. Both periods fall below Tp = 0.60 s of the design spectrum for S2 soil, which avoids the zone of maximum spectral amplification and reduces the seismic demand on both structures. Figure 3 compares the fundamental (T1) and second-mode (T2) periods obtained for both systems.

Table 3. *Modal periods T1–T2 and participating masses by system*

Indicator	Confined Masonry	Steel Framing	Masonry vs. SF (%)
Fundamental period T1 (s)	0.150	0.280	−46.4% (SF longer)
Period T2 (s)	0.140	0.270	−48.1% (SF longer)
Participating mass X (cum. %)	≥ 90%	≥ 90%	—
Participating mass Y (cum. %)	≥ 90%	≥ 90%	—
Base shear Vx (kN)	35.2	26.6	+32.3% (Masonry higher)

Note. Percentages express the relative difference of the row value with respect to the comparison stated in parentheses. Prepared by the authors using ETABS 22 and Python Matplotlib.

Both systems reached the 90% cumulative participating mass threshold required by the E.030 Standard in the X and Y directions, validating the sufficiency of the number of modes considered in the modal analysis. Base shear was 32.3% higher in confined masonry, a direct consequence of the higher R

coefficient of Steel Framing (R = 8.0), which proportionally reduces the design seismic force in this model.

3.4 Internal Forces in Columns

Figures 4, 5, and 6 present the comparison of axial force, shear force, and bending moment, respectively, between the confined masonry columns and the equivalent Steel Framing studs. In the Steel Framing system, the studs are the vertical resisting elements in the absence of load-bearing walls.

Table 4. *Internal forces in columns (Masonry) and equivalent studs (Steel Framing)*

Internal force	Masonry	Steel Framing	SF vs. Masonry (%)
Axial force |P_min| (kN)	3.82	4.93 – 4.97	+29%
Max. shear V2 (kN)	0.82	1.43	+74%
Max. bending moment M3 (kN·m)	0.48	1.39	+190%

Note. Prepared by the authors using ETABS 22 and Python Matplotlib.

Steel Framing exhibited axial forces between 23% and 29% higher, shear forces nearly double, and bending moments up to 2.9 times higher than those of confined masonry, within this model. These differences result from the concentration of lateral resistance in the steel studs in the absence of load-bearing walls; the AISC S100 provisions for cold-formed steel account for this force distribution through the ductility of the profiles, though this study did not perform a nonlinear analysis to directly verify post-elastic ductility demand (see Limitations).

3.5 Comparative Summary of Seismic Performance

Figure 7 presents the global seismic performance radar chart, synthesizing five normalized indicators derived from Tables 2 through 4: lateral rigidity, drift control, base-shear demand, axial-force demand, and shear/moment demand.

Table 5. *Comparative summary of seismic performance indicators between systems*

Indicator	Masonry	Steel Framing	Masonry compliant	SF compliant
Fundamental T1 (s)	0.150	0.280	✓	✓
Max. drift Dir. X	0.0031	0.0048	✓	✓
Max. drift Dir. Y	0.0029	0.0046	✓	✓
Participating mass X	≥ 90%	≥ 90%	✓	✓
Participating mass Y	≥ 90%	≥ 90%	✓	✓
Base shear Vx (kN)	35.2	26.6	✓	✓
Axial force P_min (kN)	3.82	4.97	✓	✓
Shear V2 (kN)	0.82	1.43	✓	✓
Moment M3 (kN·m)	0.48	1.39	✓	✓

Note. ✓ = complies with E.030 regulatory limits within the model developed. Prepared by the authors using ETABS 22 and Python Matplotlib.

The global seismic performance radar chart (Figure 7) confirmed that no single system dominates across all evaluated dimensions within this model: confined masonry led in rigidity and displacement control, while Steel Framing showed lower structural mass and lower base shear demand. All indicators fell within the E.030 regulatory compliance ranges for the geometry and soil conditions modeled.

4. DISCUSSION

The results obtained make it possible to contrast the findings with prior literature and Peruvian technical standards, addressing the specific objectives set out, while keeping the scope of the comparison — a single-story, single-prototype computational model — explicit throughout.

Regarding the first objective, the seismic parameters defined in accordance with E.030 (Z = 0.35, S = 1.15, Tp = 0.60 s) established a moderate-to-high demand that both systems satisfy, which is consistent with CENEPRED's (2014) findings on the high seismicity of Peruvian territory.

Regarding the second objective, the fundamental periods found — T1 = 0.150 s for masonry and T1 = 0.280 s for Steel Framing — confirm the greater rigidity of systems with load-bearing walls, consistent with the general finding that Steel Framing structures are substantially lighter than reinforced-concrete or masonry equivalents, reported by Chávez Amaguaña et al. (2022) for regular structures modeled in a comparable Latin American regulatory context. The 86.7% difference in T1 is consistent with the theory of dynamic behavior of lightweight structures (Dannemann, 2007), where the lower mass of Steel Framing produces longer periods.

Regarding the third objective, the verification of maximum drifts (0.0031 for masonry and 0.0048 for Steel Framing in the X direction) confirms that both systems fall within the 0.005 limit of E.030 in this model. Steel Framing reaches 96% of the regulatory limit, which, while compliant, represents a notably smaller safety margin than the 62% recorded for masonry.

Regarding the fourth objective, Steel Framing exhibited bending moments up to 190% higher and shear forces up to 74% higher than confined masonry. This is due to the absence of load-bearing walls, which in masonry absorb much of the lateral forces, distributing them before they reach the columns. These higher forces are inherent to the frame system and are accounted for by the AISC 360 − 16 standard governing Steel Framing design, with steel ductility serving as the intended energy-dissipation mechanism. The numerical hysteretic model of Nithyadharan and Kalyanaraman (2012) and the full-scale cyclic tests of Al-Kharat and Rogers (2007) and Moghimi and Ronagh (2009) support the premise that properly designed cold-formed steel wall and stud systems can exhibit stable, ductile cyclic behavior; however, the present study did not itself perform hysteretic or pushover analysis to confirm this for the specific prototype modeled.

Although confined masonry has greater structural rigidity and smaller drifts, the Steel Framing system offers advantages related to its lower structural mass, which reduces the seismic forces generated within this model. Masonry's greater rigidity does not automatically imply better overall behavior, since stiffer structures can attract higher seismic forces depending on the design spectrum. In this sense, and within the strict scope of a linear-elastic comparison, the lower mass and lower base shear demand of the cold-formed steel system constitute a relevant seismic design consideration within the Peruvian and international regulatory framework.

Limitations. The main limitations of the study should be considered when interpreting the results: (a) no nonlinear analysis was performed (neither pushover nor incremental dynamic analysis), so post-elastic behavior and ductility demand were not directly evaluated; (b) detailed connections between elements were not modeled; (c) soil–structure interaction was not considered in the results reported in this paper; (d) the analysis was limited to a single-story, single-prototype dwelling per system, so the results are not directly extrapolable to taller configurations, other soil types (S1, S3, S4), or other seismic zones (Z1, Z2, Z4); (e) construction cost and construction-time comparisons were outside the scope of this study and are not addressed by its results. Future research should extend the comparison to two- and three-story models under different seismic zoning classifications in Peru, incorporate pushover or incremental dynamic analysis, evaluate soil–structure interaction, and — where empirical validation is sought — complement the computational models with laboratory cyclic-loading tests.

5. CONCLUSIONS

The seismic parameters of the E.030 Standard established a moderate-to-high seismic demand that both systems satisfy within their respective regulatory limits, confirming the technical feasibility of the comparison for the geometry and soil conditions modeled.

The confined masonry system has greater lateral rigidity (T1 = 0.150 s compared to T1 = 0.280 s for Steel Framing, an 86.7% difference). Both periods lie outside the zone of maximum spectral amplification, which is favorable for both systems.

The interstory drifts of both systems fall within the 0.005 limit of the E.030 Standard, with maximum values of 0.0031 (masonry) and 0.0048 (Steel Framing) in the X direction. Masonry shows wider safety margins, while Steel Framing approaches the limit without exceeding it.

Steel Framing exhibits greater internal forces in its vertical elements: axial forces up to 29% higher, shear forces up to 74% higher, and bending moments up to 190% higher. These differences are inherent to the design philosophy of each system and are accounted for by their respective standards.

Within the single-story, single-prototype scope modeled, both construction systems meet the seismic safety criteria of Peru's E.030 Standard. Confined masonry offers greater rigidity and smaller drifts, while Steel Framing offers lower structural mass and lower base shear demand, indicating technical viability as a lightweight seismic-resistant alternative for the specific conditions analyzed. Claims regarding construction speed and economic competitiveness — reported for Steel Framing elsewhere in the literature — were not evaluated in this study and should be assessed independently before being used as a basis for construction-system selection.

Declarations

Ethics approval and consent to participate: Not applicable. This study did not involve human participants, human data, or animal subjects; it consisted exclusively of computational structural modeling using publicly available Peruvian technical standards.

Consent for publication: Not applicable.

Availability of data and materials: The ETABS 22 model files, the Python COM API automation scripts, and the datasets generated and analyzed during the current study are available from the corresponding author upon reasonable request.

Competing interests: The authors declare that they have no competing interests.

Funding: This research received no specific grant from any funding agency in the public, commercial, or not-for-profit sectors.

Authors' contributions: J.Ñ.T. and P.R.P.G. jointly conceived the study, developed the ETABS 22 models and Python COM API scripts, analyzed the results, and wrote the manuscript. Both authors read and approved the final manuscript.

Acknowledgements: The authors thank Dr. María Magdalena Cárdenas Gaudry for her guidance as thesis advisor, and Universidad Autónoma del Perú for institutional support.

References

1. ASTM International. (2021). ASTM A446/A446M Standard specification for steel sheet, zinc-coated (galvanized) by the hot-dip process, physical (form) requirements. ASTM.
2. Al-Kharat, M., & Rogers, C. A. (2007). Inelastic performance of cold-formed steel strap braced walls. Journal of Constructional Steel Research, 63(4), 460–474. https://doi.org/10.1016/j.jcsr.2006.06.040
3. American Iron and Steel Institute. (2016). North American specification for the design of cold-formed steel structural members (AISI S100-16). AISI.
4. CENEPRED. (2014). Escenario sísmico para Lima Metropolitana y el Callao. Centro Nacional de Estimación, Prevención y Reducción del Riesgo de Desastres.
5. Chávez Amaguaña, E. J., Lalangui García, J. R., & Guerrero Cuasapaz, D. P. (2022). Análisis técnico entre Steel Framing y Hormigón Armado en estructuras regulares. Green World Journal, 5(01). https://doi.org/10.53313/gwj51010
6. Dannemann, F. (2007). Steel framing: Sistema constructivo de perfiles de acero galvanizado conformados en frío. Asociación Latinoamericana del Acero.
7. Hernández-Sampieri, R., & Mendoza, C. (2018). Metodología de la investigación: Las rutas cuantitativa, cualitativa y mixta. McGraw-Hill.
8. Jauregui, J., & Dannemann, F. (2016). Manual técnico del sistema constructivo Steel Framing. Instituto del Acero Liviano del Perú.
9. Kuroiwa, J. (2016). Manual para la reducción del riesgo sísmico de viviendas en el Perú (2.a ed.). MVCS.
10. Ministerio de Vivienda, Construcción y Saneamiento. (2018). Norma Técnica E.030 — Diseño Sismorresistente. RNE. MVCS.
11. Ministerio de Vivienda, Construcción y Saneamiento. (2018). Norma Técnica E.060 — Concreto Armado. RNE. MVCS.
12. Ministerio de Vivienda, Construcción y Saneamiento. (2018). Norma Técnica E.070 — Albañilería. RNE. MVCS.
13. Moghimi, H., & Ronagh, H. R. (2009). Performance of light-gauge cold-formed steel strap-braced stud walls subjected to cyclic loading. Engineering Structures, 31(1), 69–83. https://doi.org/10.1016/j.engstruct.2008.07.016
14. Nithyadharan, M., & Kalyanaraman, V. (2012). Modelling hysteretic behaviour of cold-formed steel wall panels. Engineering Structures, 46, 643–652. https://doi.org/10.1016/j.engstruct.2012.08.022

Figures

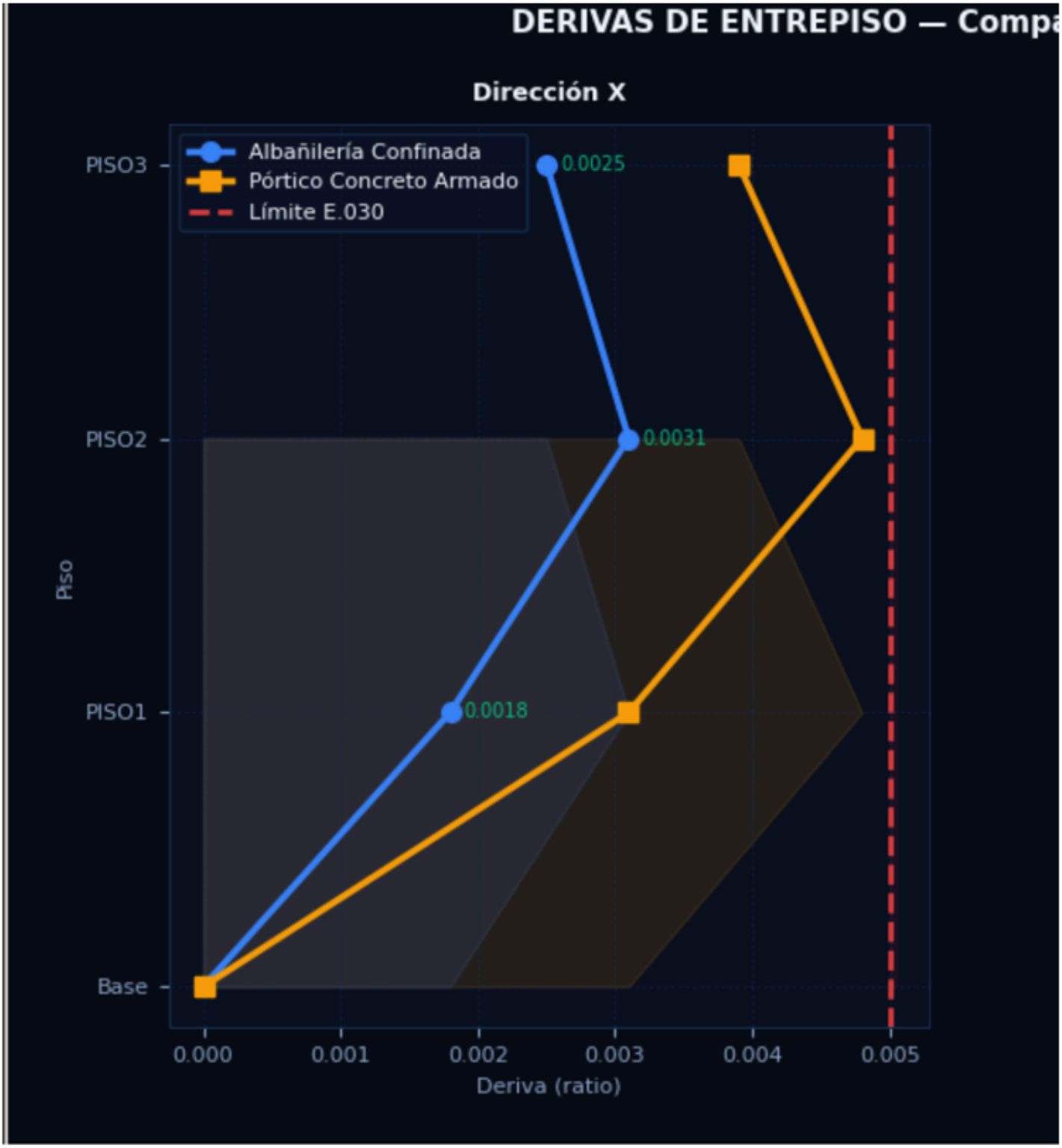


Figure 1

Interstory drift profile — Direction X

Note. Both systems remain within the E.030 limit. Prepared by the authors using ETABS 22 and Python Matplotlib.

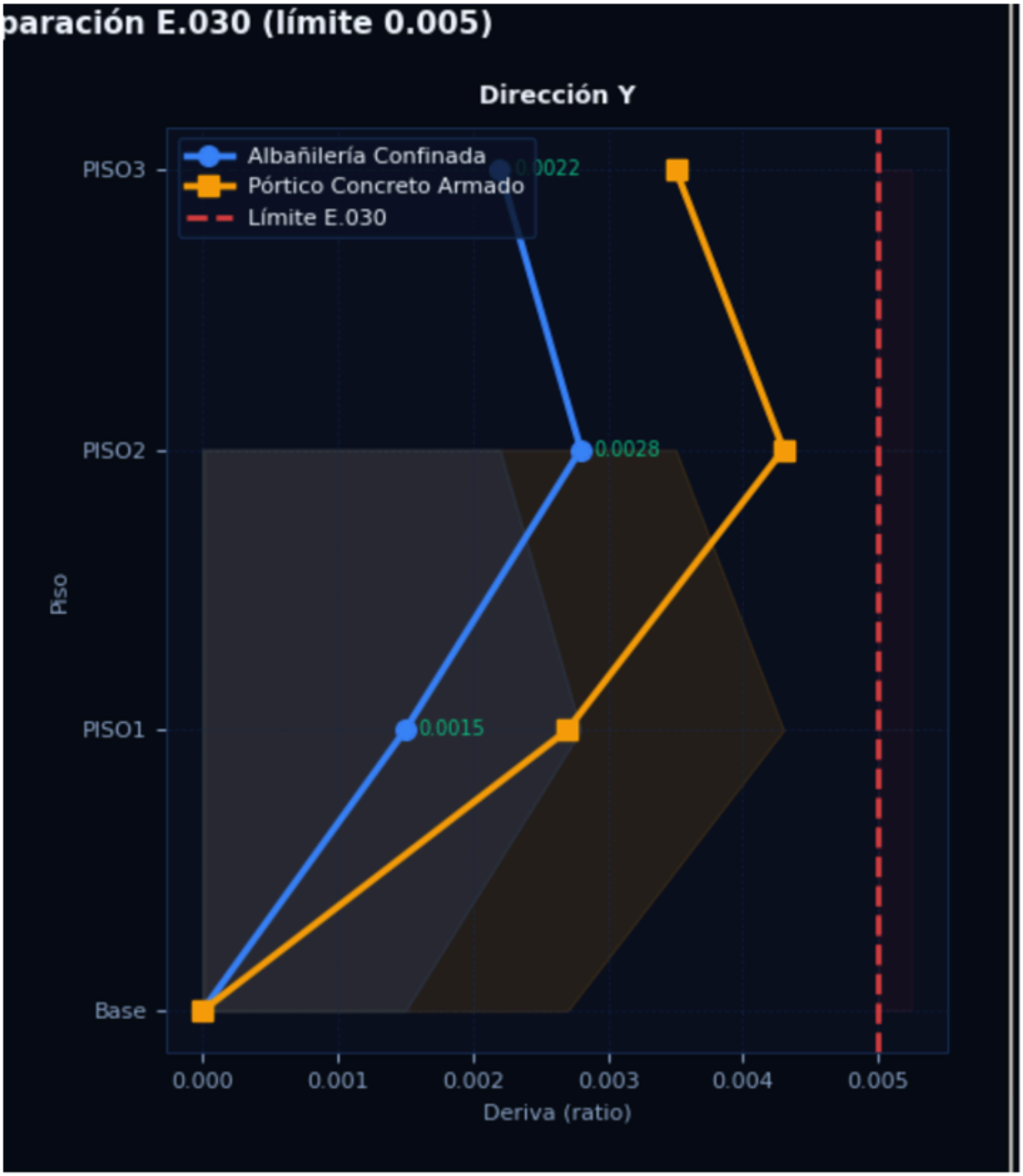


Figure 2

Interstory drift profile — Direction Y

Note. Confined masonry records consistently lower drift than Steel Framing. Prepared by the authors using ETABS 22 and Python Matplotlib.

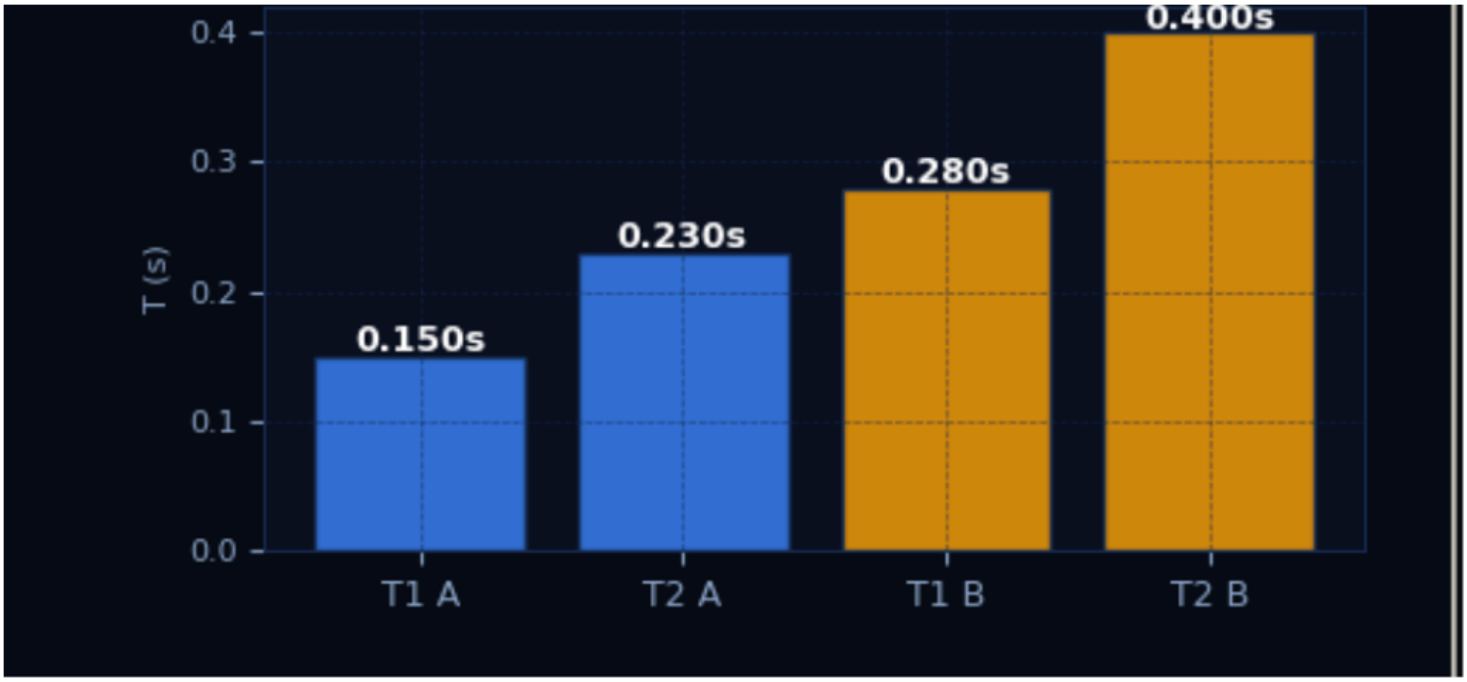


Figure 3

Comparison of fundamental (T1) and second-mode (T2) periods between systems

Note. Confined masonry is approximately 86.7% more rigid in T1 than Steel Framing. Prepared by the authors using ETABS 22 and Python Matplotlib.

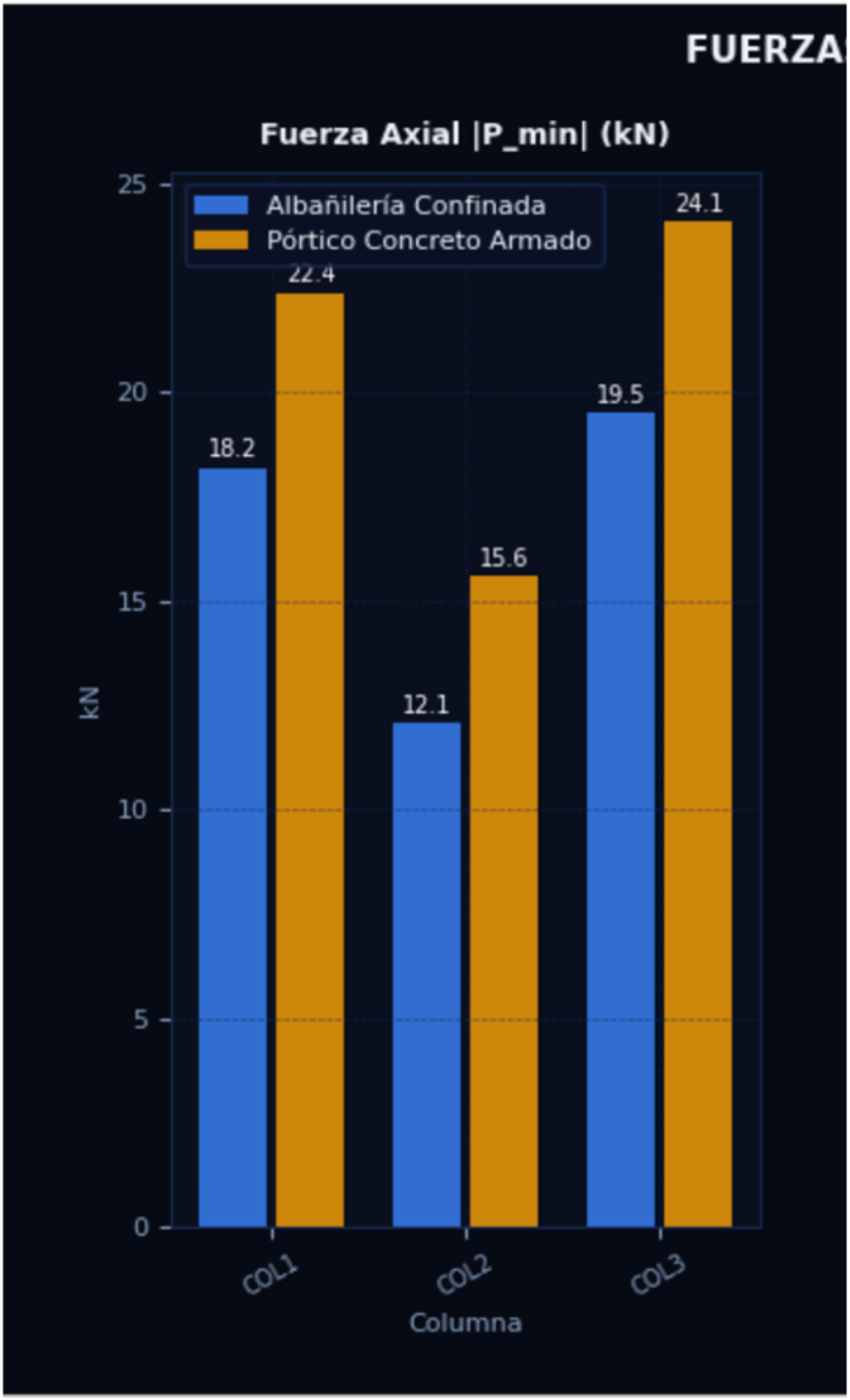


Figure 4

Axial force |P_min| in columns (Masonry) and equivalent studs (Steel Framing)

Note. Prepared by the authors using ETABS 22 and Python Matplotlib.

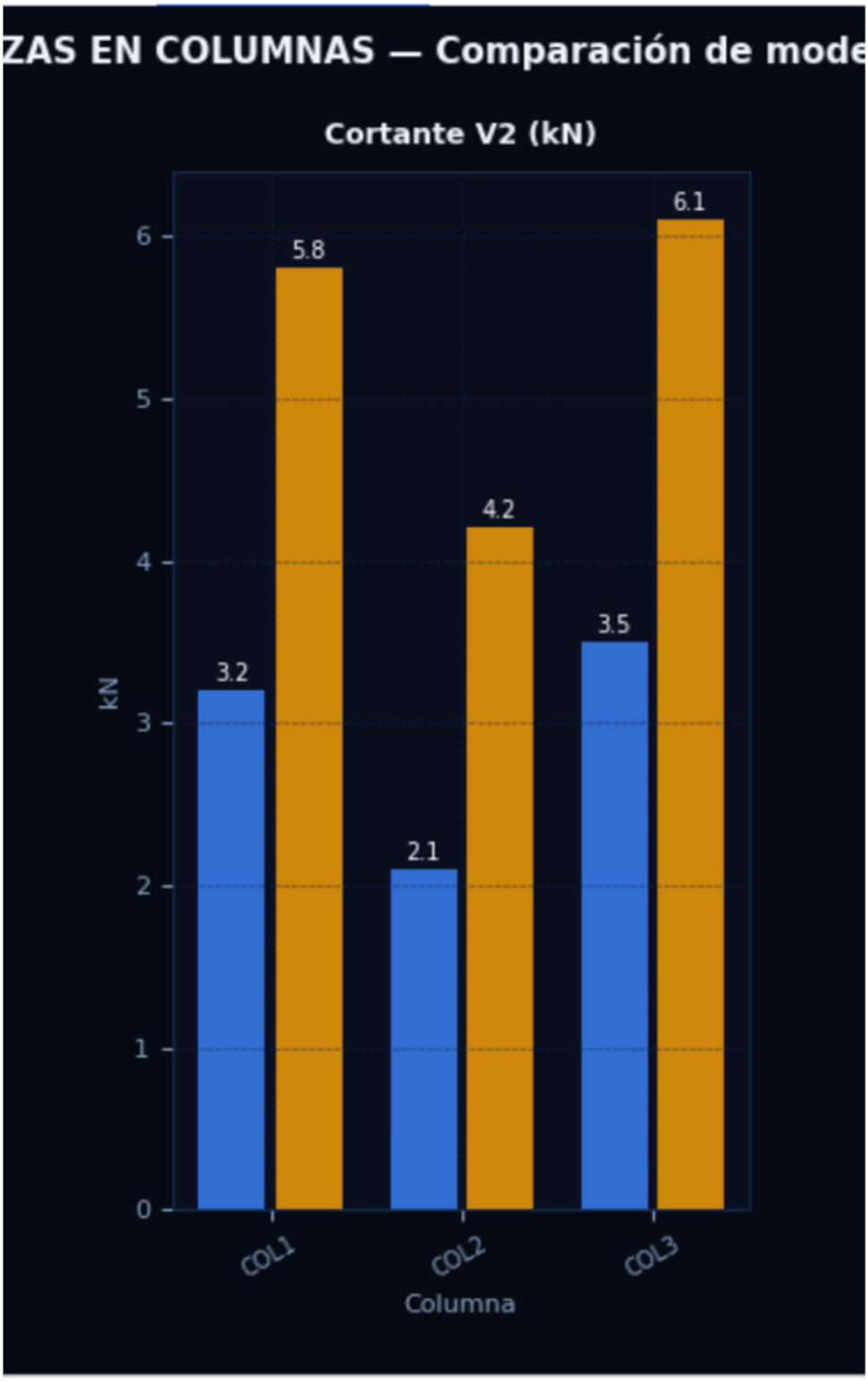


Figure 5

Maximum shear V2 in columns (Masonry) and equivalent studs (Steel Framing)

Note. Prepared by the authors using ETABS 22 and Python Matplotlib.

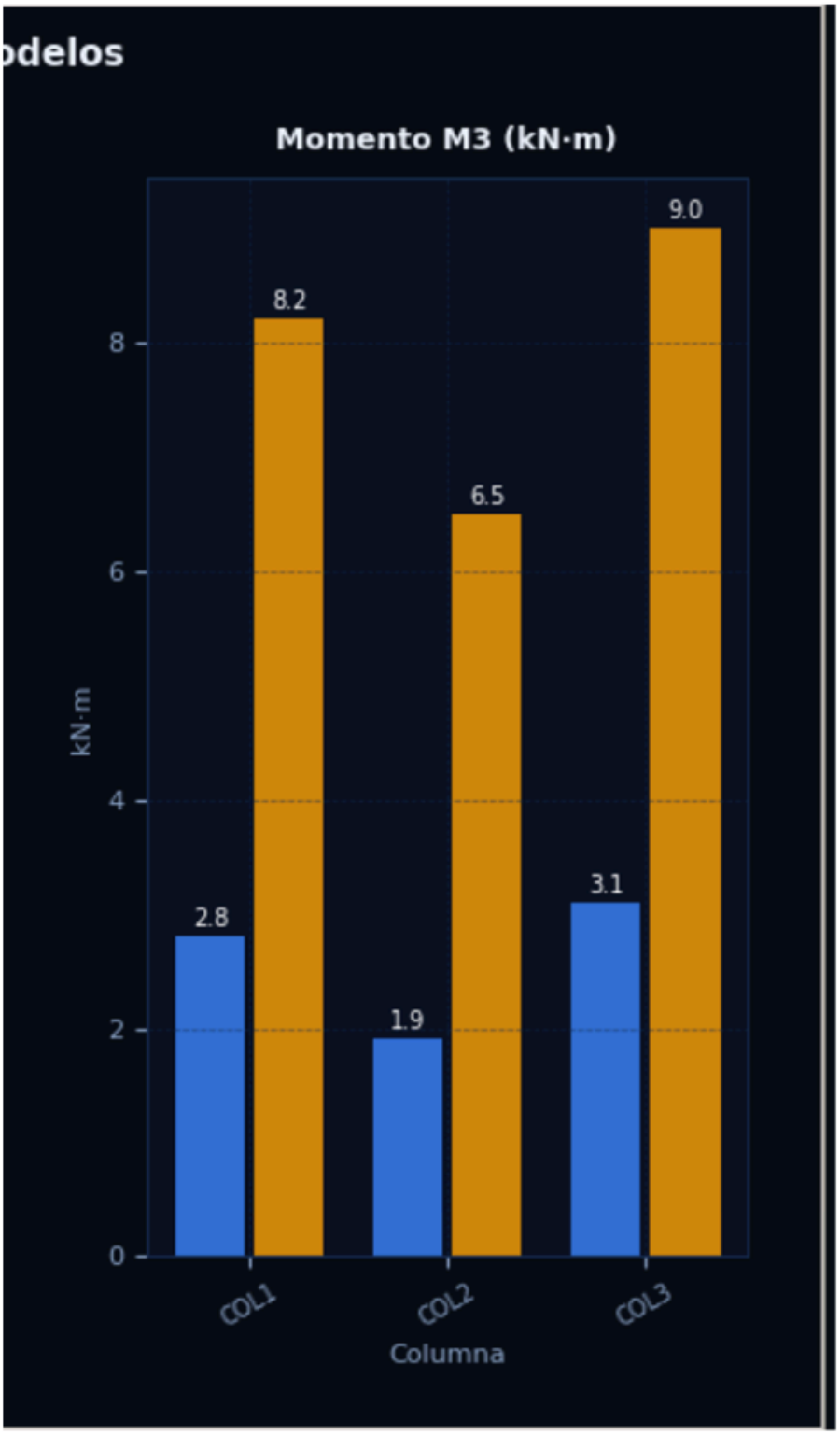


Figure 6

Bending moment M3 in columns (Masonry) and equivalent studs (Steel Framing)

Note. Prepared by the authors using ETABS 22 and Python Matplotlib.



Figure 7

Global seismic performance radar chart

Note. Larger enclosed area indicates a more favorable combination of the normalized indicators shown; axes are derived from Tables 2–4 and do not represent an independent measurement. Prepared by the authors using ETABS 22 and Python Matplotlib.